New Phytologist

The DNA-dependent protease AtWSS1A suppresses persistent double strand break formation during replication

Leonie Hacker iD**, Niklas Capdeville** iD**, Laura Feller, Janina Enderle-Kukla** iD**, Annika Dorn** iD **and Holger Puchta** iD

Botanical Institute, Molecular Biology and Biochemistry, Karlsruhe Institute of Technology, Fritz-Haber-Weg 4, Karlsruhe 76131, Germany

Author for correspondence:
Holger Puchta
Email: holger.puchta@kit.edu

Summary

- The protease WSS1A is an important factor in the repair of DNA-protein crosslinks in plants.
- Here we show that the loss of WSS1A leads to a reduction of 45S rDNA repeats and chromosomal fragmentation in Arabidopsis. Moreover, in the absence of any factor of the RTR (RECQ4A/TOP3α/RMI1/2) complex, which is involved in the dissolution of DNA replication intermediates, WSS1A becomes essential for viability.
- If WSS1A loss is combined with loss of the classical (c) or alternative (a) nonhomologous end joining (NHEJ) pathways of double-strand break (DSB) repair, the resulting mutants show proliferation defects and enhanced chromosome fragmentation, which is especially aggravated in the absence of aNHEJ. This indicates that WSS1A is involved either in the suppression of DSB formation or in DSB repair itself. To test the latter we induced DSB by CRISPR/Cas9 at different loci in wild-type and mutant cells and analyzed their repair by deep sequencing. However, no change in the quality of the repair events and only a slight increase in their quantity was found.
- Thus, by removing complex DNA-protein structures, WSS1A seems to be required for the repair of replication intermediates which would otherwise be resolved into persistent DSB leading to genome instability.

Introduction

DNA, the fundamental basis of life, is constantly being damaged by a variety of environmental and endogenous sources, thereby compromising the integrity of the genome. Among this DNA damage, DNA double-strand breaks (DSBs) and crosslinks within DNA or with proteins are among the most toxic lesions, as they pose a severe obstacle to replication, transcription and cell division machineries, thus leading to the loss of genetic information, chromosomal rearrangements or even cell death. To maintain DNA integrity, plants have evolved a vast toolbox of specialized proteins, each of which contributes with its own special features to DNA repair. DNA-protein crosslinks (DPCs) are arguably among the most complex of this type of damage, as they can vary greatly in their physicochemical properties. They differ in terms of the type of protein entrapped, the crosslink binding, or even the presence and type of DNA strand break adjacent to the DPC (Ide *et al.*, 2011). Therefore, complete repair requires different, consecutive mechanisms. The first step of damage control, resolution of the DPC, involves proteases for degradation of the protein moiety or endonucleases for DNA cleavage. However, after resolution of the DPC, secondary damage occurs, ranging from smaller bulky DNA adducts to DSB which must be repaired downstream by other canonical DNA repair mechanisms, such as nucleotide excision repair, translesion synthesis,

nonhomologous end joining (NHEJ) or homologous recombination (HR) (Stingele *et al.*, 2017).

Just recently, pathways of DPC repair were characterized in plants (Enderle *et al.*, 2019b; Hacker *et al.*, 2020). A central role in DPC repair is occupied by the metalloprotease WSS1A. CRISPR/Cas-generated *wss1A* Arabidopsis mutants showed a fasciated phenotype, short roots, reduced fertility and enhanced sensitivity against the DPC-inducing genotoxins Camptothecin (CPT), Etoposide (Eto) and Cisplatin (Enderle *et al.*, 2019a; Hacker *et al.*, 2021). If the DPC is not removed in time, this can lead to replication fork collapse and the formation of a one-sided DSB (Vaz *et al.*, 2016). However, DSB also arise as intermediates of efficient DPC repair pathways. This might be the case when the DPC was located next to a DSB. A second possibility is the processing by endonucleases, such as MUS81, which is working in parallel to WSS1A.

For the repair of DSB, two main pathways exist: NHEJ and HR. Homologous recombination is the more precise way of repair, as the missing genetic information is copied from a suitable template, such as a sister chromatid, the homologous chromosome or another homologous sequence. During classical HR, which is also used during meiosis, one end of the damaged DNA strand invades the homologous template, searches for homologies and then copies the missing genetic information by forming a displacement loop (D-loop). The discarded strand can be

captured by the second end of the damaged strand, followed by repair synthesis and ligation of DNA ends (Schröpfer *et al.*, 2014a). The resulting structure is called a double Holliday junction (dHJ) and can be resolved by different mechanisms (Szostak *et al.*, 1983; Knoll & Puchta, 2011). A prominent way is the dissolution of the dHJ by the conserved RTR (RECQ4A/TOP3α/RMI1/2) complex, which consists of the helicase RECQ4A, the topoisomerase TOP3α and the structural proteins RMI1 and RMI2 in Arabidopsis (Knoll *et al.*, 2014). For dissolution of the dHJ, RECQ4A pushes the two junction points towards each other, thereby forming a hemicatenane which can then be cleaved by TOP3α (Plank *et al.*, 2006; Raynard *et al.*, 2006; Hartung *et al.*, 2008). The outcome of this process is always a noncrossover product (Wu & Hickson, 2003; Hartung *et al.*, 2008). However, the dHJ can also be resolved by endonucleases, such as MUS81, and this can result in noncrossover as well as crossover products, depending on the cutting orientation. In addition to its function in dHJ dissolution, the RTR complex is also involved in the processing of several other types of putative replication blocks, such as G4 structures.

However, in multicellular organisms, such as plants, error-prone NHEJ is the preferred pathway for DSB repair (Sargent *et al.*, 1997). At least two different ways of NHEJ exist: classical NHEJ (cNHEJ) and alternative NHEJ (aNHEJ). In cNHEJ, the KU70/KU80 heterodimer binds to the ends of the DSB to prevent resection of the DNA and then the ligase LIG4 can directly seal the gaps. This process mostly results in perfect repair of the DSB but sometimes causes small deletions or insertions (Schmidt *et al.*, 2019; Zhao *et al.*, 2020). Most DSBs are repaired by cNHEJ, but during the S and G2 phases of the cell cycle there is a higher rate of aNHEJ because, then, factors that promote extensive resection of DSB ends are more active (Ira *et al.*, 2004; Chang *et al.*, 2017). During resection of the 5′ ends of the DSB, microhomologies are exposed in the 3′ overhangs which can subsequently anneal with each other. After removal of the nonhomologous 3′ flaps, the key enzyme of aNHEJ – POLQ, which harbors a polymerase as well as a helicase domain – fills the gaps by extending the 3′ ends surrounding the microhomologies. These are then sealed by specific ligases (Arana *et al.*, 2008; Liang *et al.*, 2008; Chan *et al.*, 2010; Seol *et al.*, 2018). As both aNHEJ and HR require resected ends, the two DSB repair mechanisms compete for the same substrate (Schrempf *et al.*, 2021). However, the repair of DSB by aNHEJ is highly error-prone and results in larger deletions or in templated insertions (van Schendel *et al.*, 2016).

In plants, a homolog of POLQ could be identified, named TEBICHI, hereafter referred to as AtPOLQ. This was shown to be important in cell cycle regulation, cell differentiation and recombination. *teb* mutants display enhanced sensitivity against the genotoxins MMS, MMC and Cisplatin, thus indicating that AtPOLQ is an important factor in maintaining genome integrity in plants (Inagaki *et al.*, 2006; Klemm *et al.*, 2017; Nisa *et al.*, 2021) Moreover, AtPOLQ is important for T-DNA integration (van Kregten *et al.*, 2016; Nishizawa-Yokoi *et al.*, 2021).

As the RTR complex and the NHEJ pathways are central for safeguarding genome stability in plants, we aimed to investigate the relationships of these factors to the central DPC repair protease WSS1A. Our studies reveal that WSS1A has a surprisingly crucial role in the removal of aberrant replication intermediates in Arabidopsis that would otherwise result in persistent DSB.

Methods

Plant lines and cultivation conditions

All plant lines used in this study were from the Columbia (Col-0) ecotype of *Arabidopsis thaliana*. The CRISPR/Cas9-generated *wss1A-3* mutant as well as the T-DNA insertion mutants *recq4A-4* (GABI_203C07), *rmi1-2* (SALK_094387), *rmi2-1* (GABI_148E03), *top3α-2* (GABI_476A12), *teb-5* (SALK_018851) and *lig4-3* (SALK_095962) have been described previously (Inagaki *et al.*, 2006; Hartung *et al.*, 2007, 2008; Waterworth *et al.*, 2010; Recker *et al.*, 2014; Röhrig *et al.*, 2016; Dorn *et al.*, 2018; Enderle *et al.*, 2019a). Double mutants were generated by crossbreeding of the respective single mutant lines. The homozygous double mutants were identified in the F₂ generation by PCR-based genotyping, using wild-type (WT) and T-DNA-specific primer combinations (Supporting Information Tables S1, S2). For reproduction and phenotyping purposes, plants were cultivated in the glasshouse in soil using a 1 : 1 mixture of Floraton (Floragard, Oldenburg, Germany) and vermiculite (2–3 mm; Deutsche Vermiculite Dämmstoff, Sprockhövel, Germany) at 22°C and 16 h : 8 h, light : dark conditions. For root and sensitivity assays, plants were grown under axenic conditions. Therefore, seeds were surface-sterilized with a 4% sodium hypochlorite solution and stratified overnight at 4°C. On the next day, the seeds were sown on germination media (GM: 4.9 g l⁻¹ Murashige & Skoog medium (Duchefa, Haarlem, the Netherlands), 10 g l⁻¹ sucrose, pH 5.7, with potassium hydroxide) and incubated in a plant tissue chamber (CU-36L4; Percival Scientific, Perry, IA, USA) with a stable temperature of 22°C and 16 h : 8 h, light : dark conditions.

Analysis of somatic anaphases

For analysis of defects in somatic anaphases, cells from flower buds were prepared as previously described (Ross *et al.*, 1996).

Quantitative real-time PCR

For quantification of the relative 45S rDNA repeat amount, quantitative real-time PCR (qPCR) analyses with specific primer combinations (Table S3) for amplification of the 18S, 25S and 5.8S genes was performed as previously described (Röhrig *et al.*, 2016; Dorn *et al.*, 2019). Genomic DNA of 2-wk-old *Arabidopsis* plantlets, grown under axenic conditions was used as a template. A reaction volume of 10 μl was chosen: 5 μl KAPA SYBR FAST Mastermix (VWR International, Darmstadt, Germany), 200 nM each of both primers, 3.8 μl ddH₂O and 1 μl template (0.25 ng). The analysis was performed using a LightCycler 480 (Roche Diagnostics, Mannheim, Germany). The single-copy gene *Ubiquitin 10* was used for normalization.

Fluorescence *in situ* hybridization

For cytological quantification of the 45S rDNA area, fluorescence *in situ* hybridization (FISH) was performed as described previously (Röhrig *et al.*, 2016). Microscopic images were taken using the same parameters. The area of the 45S rDNA probe signals was determined via IMAGEJ, using the 'rolling ball' algorithm for background subtraction and a threshold of 16 standard deviations. Analysis was performed in independent triplicates and at least 20 individual nuclei per replicate were analyzed.

Embryo analysis

To analyze the vitality of embryos in Arabidopsis plants, 10 large immature green siliques of each genotype were harvested from at least three 8-wk-old plants each. The siliques were opened with a small cannula (Sterican 0.45 × 25 mm; B. Braun SE; Melsungen, Germany) and all embryos inside were extracted onto a white cloth. All seeds of each silique were counted by use of a binocular, distinguishing between brownish/defective and greenish/healthy embryos. Depicted is the mean value of the percentage of defective seeds per silique of 10 siliques per genotype.

Root length assay

To determine root lengths of the different mutant lines, surface-sterilized and stratified seeds were sown on plates with solid GM (1% agar) and incubated vertically in a plant tissue chamber for 9 d. Afterwards, the plantlets were photographed on a black background. The root length was subsequently measured using the SmartRoot add-on of IMAGEJ (Lobet *et al.*, 2011). Displayed are the relative means of three technical replicates of seven roots each.

Analysis of cell death in root tips upon Eto treatment

To investigate the sensitivity to Eto, the number of dead cells in the root tips of different mutant lines was determined untreated and after treatment with Eto. For this purpose, the roots were stained with propidium iodide (PI). To grow the roots, surface-sterilized, stratified seeds were sown on square plates containing GM solid medium (1% agar) and then incubated in an upright position in a plant tissue chamber for 4 d. For treatment with Eto, the seedlings were transferred to a six-well plate. Each well contained 4 ml of GM liquid medium. Then 1 ml of the Eto solution, diluted in GM liquid medium, was added to obtain a final concentration of 20 µM (stock solution 50 mM, solved in dimethyl sulfoxide). For comparison, untreated roots were analyzed and transferred directly into 5 ml GM liquid medium. After another 24 h incubation step in the plant tissue chamber, the seedlings were washed with double-distilled water and then placed on a slide containing PI solution (5 µg ml^{-1}). Using a confocal laser scanning microscope (LSM 700 Laser Scanning Microscope; Carl Zeiss Microscopy, White Plains, NY, USA), the dead cells (visible as PI-stained sectors) in the root meristem in the anterior 200 µm of the root tip were counted. Displayed are the mean values of three biological replicates.

Fertility analysis

To analyze the fertility of the different mutant lines, five mature siliques per genotype were harvested from at least five 8-wk-old Arabidopsis plants and incubated in 70% ethanol for 24 h. Subsequently, the seeds in the now transparent siliques were counted with the help of a binocular microscope.

T-DNA constructs

T-DNA constructs used in this study are based on the previously described pDe-Sa-Cas9, pDe-Sp-Cas9, pEn-Sp-Chimera and pEn-Sa-Chimera plasmids (Fauser *et al.*, 2014; Steinert *et al.*, 2015). Spacer sequences for the three targets were cloned into individual pEn-Sa-Chimera entry vectors as previously described (Fauser *et al.*, 2014). The specified sgRNA expression cassettes were transferred into pDe-Sa-Cas9 destination vectors via a Gateway LR reaction. Sequences of the used oligonucleotides are listed in Table S4. Arabidopsis plants were transformed via floral dip using the Agrobacterium strain GV3101, as previously described (Clough & Bent, 1998).

Amplicon deep sequencing

T1 plants were grown on GM with cefotaxime (500 mg l^{-1}) and kanamycin (30 mg l^{-1}) as selection marker. DNA was extracted from batches of 40 plants after 2 wk of incubation, as described previously (Fulton *et al.*, 1995). Amplicons with universal adapter sequences were generated with 30 ng of genomic DNA using a proof-reading polymerase. Sequences of the oligonucleotides used are listed in Table S5. Illumina paired-end sequencing was performed by Eurofins Genomics Germany GmbH. Data analysis was performed using CRISPRESSO2 (Clement *et al.*, 2019) with default settings, CRISPR RGEN TOOLS CAS-ANALYZER (comparison range (R) = use both ends, minimum frequency (n) = 1 and no WT marker (r); Park *et al.*, 2017), R and EXCEL.

Calculation of statistical significances

To determine statistical differences in the number of defective anaphases and of defective embryos in the different genotypes, a two-sided Fisher's exact test was used. The two-sided t-test with unequal variances was used to determine statistical differences in root length assays, fertility analyses and qPCR. A two-way ANOVA with subsequent Tukey's multiple comparison was used to determine statistical differences in the number of dead cells per root. Statistical differences are presented as $a \neq b$ when $P < 0.05$.

Accession numbers

Further information and gene sequences of the proteins described in this study can be found in The Arabidopsis Information Resource (https://www.arabidopsis.org/) with the following accession numbers: *WSS1A*, At1g55915; *RECQ4A*, At1g10930;

RMI1, At5g63540; *RMI2*, At1g08390; *TEBICHI*, At4g32700; *TOP3α*, At5g63920; *LIG4*, At5g57160.

Results

WSS1A loss leads to enhanced chromosome fragmentation and a loss of genomic 45S rDNA repeats

By implementing sensitivity assays using crosslinking agents and topoisomerase inhibitors to CRISPR/Cas knockout mutants, we were able to define that WSS1A is required for various kinds of enzymatic as well as nonenzymatic DPCs (Enderle *et al.*, 2019a; Hacker *et al.*, 2021). To further define the direct consequences of WSS1A loss on the integrity of the genome, we determined whether its mutation results in an accumulation of chromosomal aberrations in the anaphase or in a change in the number of 45S rDNA repeats in Arabidopsis.

The analysis of mitotic anaphases allows the visualization of different kinds of chromosomal instabilities, namely anaphase bridges and chromosome fragmentations. Anaphase bridges arise mainly as a result of defects during DNA replication, whereas fragmented chromosomes are an indication of deficiencies in DSB repair. We counted chromosomal aberrations occurring in somatic anaphases in a well-characterized CRISPR/Cas knockout mutant of *WSS1A* (Enderle *et al.*, 2019a). For the classification of an anaphase bridge, a connection of the two chromosome groups had to be visible, while fragments were classified by the presence of chromatin outside of the two groups without a connection. Surprisingly, the *wss1A-3* line showed a significantly increased number of defective anaphases, which was about four times higher than in the WT (Fig. 1a). Although the number of anaphase bridges was similar to the WT, the detected increase was solely a result of chromosome fragmentation. Thus, WSS1A is required for DSB avoidance, either by being directly involved in its repair process or by suppression of DSB formation.

Owing to its high transcription rate as well as its arrangement in tandem arrays, the 45S rDNA represents one of the most unstable regions of the genome. For important replicative DNA repair factors, such as RTEL1, RMI2 or FANCJB, an involvement in the stabilization of ribosomal DNA (rDNA) repeats has already been described in Arabidopsis (Röhrig *et al.*, 2016; Dorn *et al.*, 2019). Thus, deficiencies in replicative DNA repair might be correlated with a loss of 45S rDNA repeats. In Arabidopsis, the 45S rDNA localizes within nucleolus organizer regions on chromosomes II and IV and encodes the 18S, 5.8S and 24S rRNA genes. For the determination of relative 45S rDNA copy number, gDNA of 2-wk-old *wss1A-3* and WT plantlets was analyzed by qPCR using specific primer combinations (Röhrig *et al.*, 2016; Dorn *et al.*, 2019) to amplify the individual rRNA genes. For all three 45S rRNA genes, WSS1A-deficient plants showed a drastically reduced copy number of about half compared with WT plants (Fig. 1b). Subsequent FISH analyses using an Atto488-labeled 45S rDNA-specific probe, as described previously (Röhrig *et al.*, 2016), validated the results (Fig. 1c). This indicates that WSS1A is required for rDNA maintenance by, most probably, safeguarding proper DNA replication of the tandem repeats.

Simultaneous loss of WSS1A and factors of the RTR complex results in embryo lethality

The RTR complex and its components are required for dissolving aberrant DNA replication and recombination intermediates in Arabidopsis. In some cellular processes, only individual factors of the RTR complex are involved. However, other repair pathways require the whole complex which is also documented by the fact that the knockout of different factors leads to different defects in somatic growth and meiosis (Hartung *et al.*, 2008; Röhrig *et al.*, 2016; Dorn *et al.*, 2018). To reveal the functional relationship of WSS1A with components of the RTR complex, we crossed the respective single mutants (*wss1A-3* with *recq4A-4*, *top3α-2*, *rmi1-2* and *rmi2-1*) of *Arabidopsis* in order to generate the corresponding double mutant lines (Hartung *et al.*, 2007, 2008; Röhrig *et al.*, 2016; Dorn *et al.*, 2018; Enderle *et al.*, 2019a). In the F_2 generation, where by Mendelian segregation double mutants should arise at a ratio of 1 : 16, we screened at least 40 plants per genotype. However, no homozygous double mutant line was found. To increase the chance of finding a double mutant in the next generation, we propagated lines that were heterozygous in one factor and homozygous in the other. As *wss1A* single mutants already exhibit a strong phenotype, we preferentially chose *WSS1A* as the heterozygous factor and the RTR complex factors as the homozygous ones, except in the case of the sterile *top3α* mutant. However, after screening of at least 80 plants in the F_3 generation, we still could not find a homozygous double mutant line, although all plants growing on a plate were screened, including very small, poorly growing plants. As we did not observe the expected Mendelian segregation, we wondered at which developmental stage the missing double mutants might have died.

To address this question, we harvested 10 large, still immature, siliques of the *recq4A-4−/−* *wss1A-3+/−* mutants, the corresponding single mutants and the WT and compared the embryos they contained. In the *recq4A-4−/−* *wss1A-3+/−* siliques, 25% of the embryos were brownish and deformed, whereas the WT and *recq4A-4* contained only greenish, healthy embryos (Fig. 2b). The heterozygous *wss1A-3* mutant contained an increased proportion of defective embryos at *c.* 5%, again indicating the great impact of WSS1A on cell viability. In order to support these findings, we repeated the experiment with *rmi1-2−/−* *wss1A-3+/−* plants and obtained comparable results (Fig. S1). A further analysis of embryo development in *rmi1-2+/−* *wss1A-3−/−* siliques confirmed problems in embryo development with a large number of seeds containing defective or lacking embryos (Fig. S2). Our results indicate that the simultaneous loss of WSS1A and any of the RTR complex factors results in embryo lethality.

WSS1A and LIG4 work in parallel pathways in the repair of Topoisomerase 2 cleavage complexes

As our results hint at the presence of unrepaired DSBs in the absence of WSS1A and as NHEJ is the main mechanism for DSB repair in somatic plant cells, it was important to uncover the interplay of these pathways. We generated two different double mutant lines with *wss1A-3*, one with the cNHEJ mutant *lig4-*
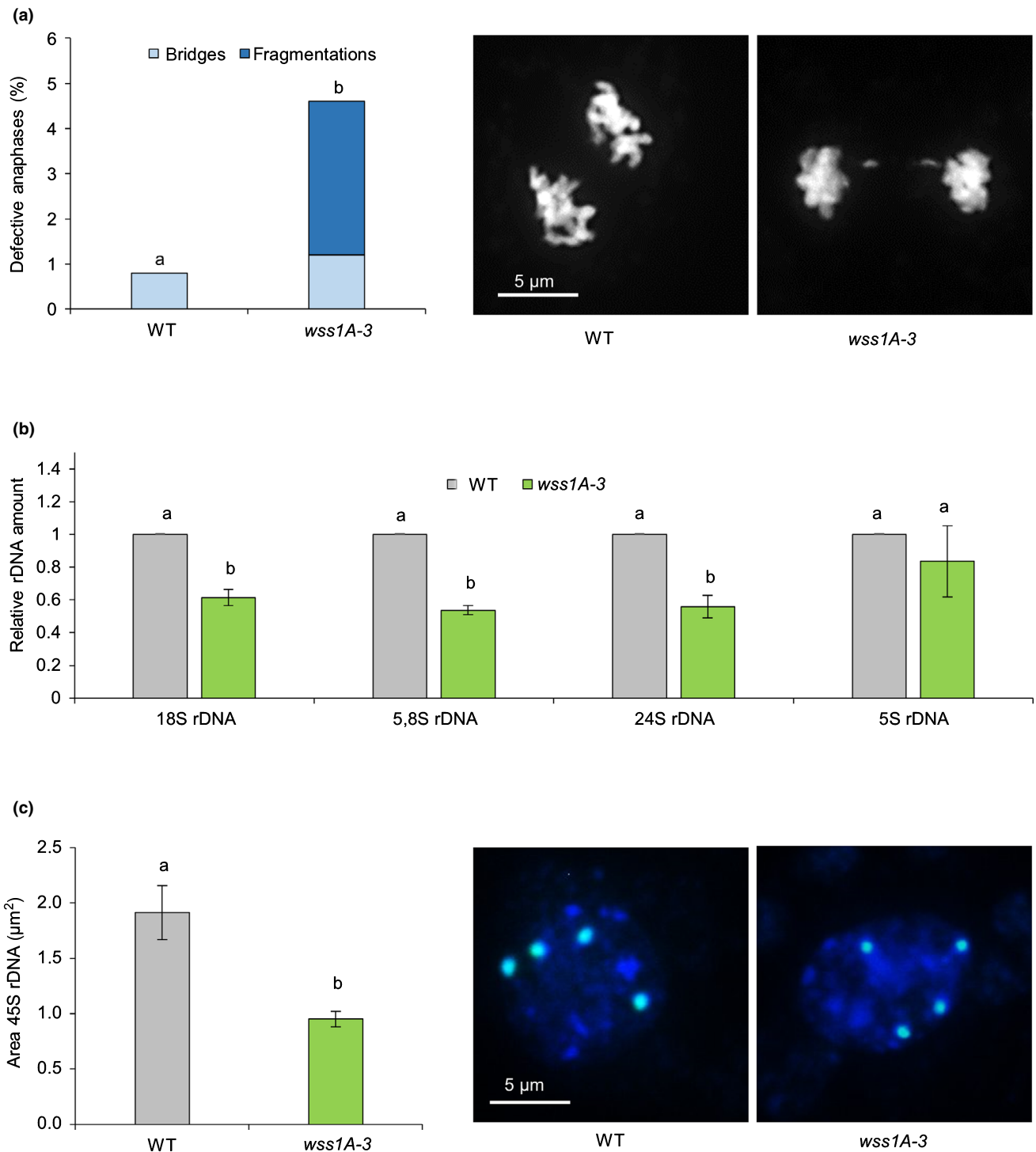
Fig. 1 Characterization of *Arabidopsis thaliana wss1A-3* in somatic cell division and rDNA amount. (a) Somatic anaphases of the wild-type (WT, $n = 250$) and the *wss1A-3* mutant line ($n = 352$). Chromatin spreads were stained with 4′,6-diamidino-2-phenylindole (DAPI) and visualized by epifluorescence microscopy. Defects were subdivided into anaphase bridges and chromosomal fragmentations. The *wss1A-3* single mutant showed significantly more defective anaphases than did the WT, most of which were chromosomal fragmentations. Statistical differences were calculated using a two-tailed Fisher's exact test. (b) Using quantitative real-time (qPCR) analyses with specific primer pairs to amplify the individual 45S rRNA genes, a significantly reduced 45S rDNA repeat content of *wss1A-3* (up to 39%) was detected compared with WT plants ($n = 3$, $n = 5$). Statistical differences were calculated using a two-tailed *t*-test with unequal variances. (c) Fluorescence *in situ* hybridization (FISH) analyses with specific Atto488-labeled 45S rDNA probes and DAPI staining of chromatin confirmed the observed rDNA loss of the *wss1A-3* mutant ($n = 3$, $n = 20$). Statistical differences were calculated using a two-tailed *t*-test with unequal variances and are presented as $a \neq b$ when $P < 0.05$. Error bars represent the standard deviation between the mean values of three biological replicates. *n*, number of biological repeats; *N*, samples per biological repeat.
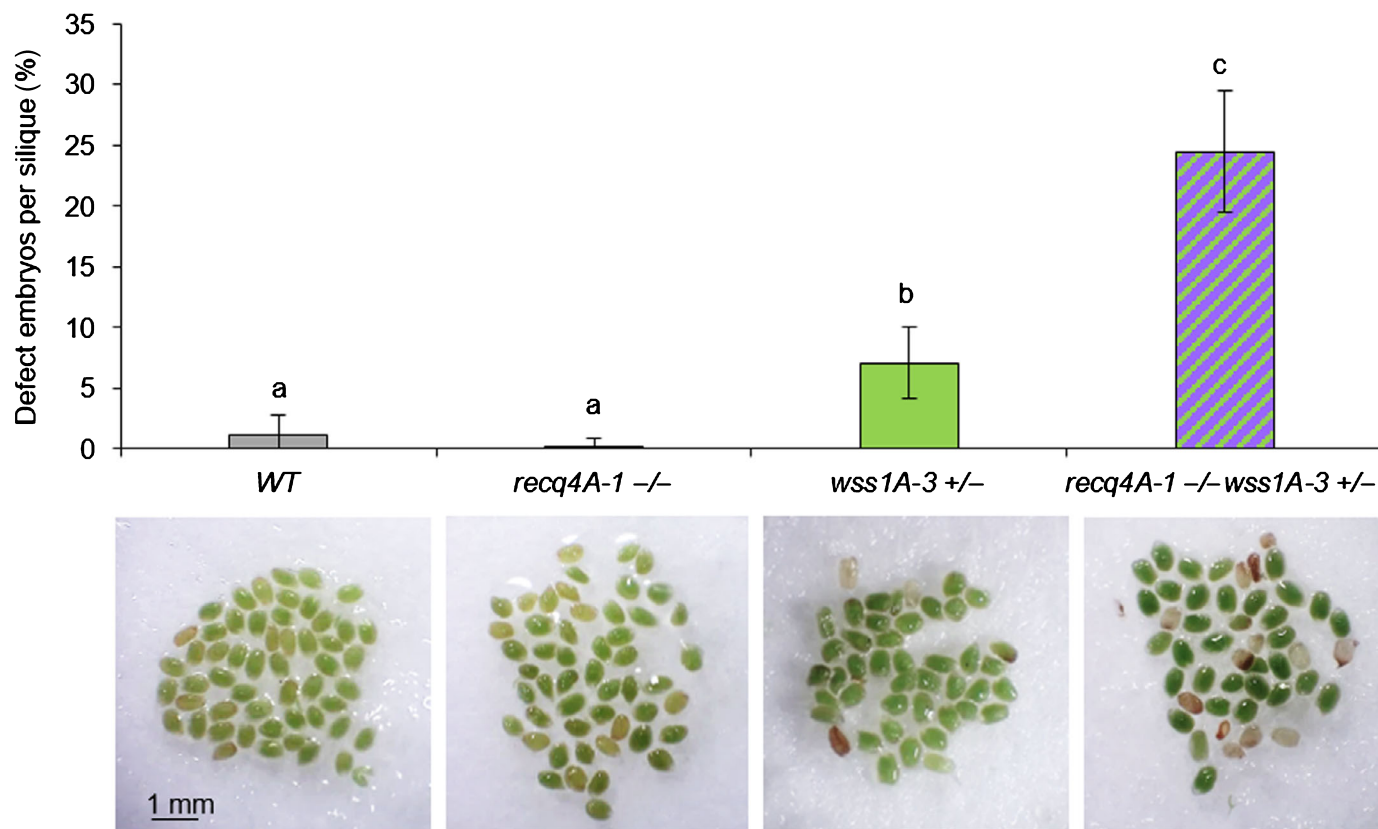
Fig. 2 Double mutants with simultaneous deficiency in WSS1A and in factors of the RTR (RECQ4A/TOP3α/RMI1/2) complex are embryo-lethal. Means of the percentage of defective embryos per immature silique of *c*. 8-wk-old *Arabidopsis thaliana* plants (*n* = 1, *n* = 10). The heterozygous *recq4A-4−/−wss1A-3+/−* double mutant line contained *c*. 25% defective embryos per silique, which correlates with the expected number of homozygous double mutants according to Mendelian segregation. Statistical differences were calculated using a two-tailed *t*-test with unequal variances and are presented as *a* ≠ *b* when *P* < 0.05. Error bars represent the standard deviation between the 10 different siliques of each genotype. *n*, number of biological repeats; *N*, samples per biological repeat.

5 and one with the aNHEJ mutant *teb-5* (Inagaki *et al.*, 2006; Waterworth *et al.*, 2010). Homozygous double mutant lines were identified in the F₂ generation by PCR-based genotyping.

The *lig4-5 wss1A-3* mutant displayed no difference in germination rate and in its growth phenotype in comparison to the *wss1A-3* mutant (Fig. 3a). However, subsequent analysis of the root length revealed that the double mutant exhibits statistically significant shorter roots than both single mutants (Fig. 3b). The root meristem represents a rapidly dividing tissue and is thus extremely sensitive to replicative stress. As the *lig4-5 wss1A-3* double mutant line exhibited a synergistic effect with a strongly reduced root length, this indicates that cNHEJ and WSS1A are involved in independent DNA repair pathways to safeguard cell proliferation.

Topoisomerase 2 cleavage complexes (TOP2cc) represent a specific kind of DPC, as they are associated with a DSB. Topoisomerase 2 (TOP2) is an essential enzyme in every living organism as it decatenates DNA by the insertion of a DSB and the subsequent passage of an intact DNA duplex through the DSB. However, the reaction intermediate, in which TOP2 is linked with two 5′ phosphodiester-bonds to the ends of a DSB, can be trapped spontaneously or after treatment with the topoisomerase inhibitor Eto. To analyze whether cNHEJ and WSS1A work in parallel in TOP2cc repair, we performed a sensitivity assay by

counting the number of dead cells from roots treated with 20 µM Eto compared with untreated roots after staining with PI. Propidium iodide is a fluorescent dye that selectively permeates the membrane of dead cells and, thus, can be used to distinguish between dead and living cells. The *lig4-5* and the *wss1A-3* single mutant line exhibited a significantly enhanced number of dead cells upon treatment with Eto compared with WT plants, indicating that both factors are involved in TOP2cc repair (Fig. 3c). The increase in dead cells in the *wss1A-3* mutant after treatment with Eto compared with untreated plants was about three dead cells, while the *lig4-5* mutant showed an increase of about eight dead cells after treatment with Eto. This indicates that cNHEJ is even more important for the repair of TOP2cc than is WSS1A. As the *lig4-5 wss1A-3* double mutant showed significantly more dead cells than both single mutant lines, it can be concluded that cNHEJ and WSS1A are working in parallel pathways in TOP2cc repair.

Loss of WSS1A and the aNHEJ factor AtPOLQ results in severe growth defects

Next, we characterized the *teb-5 wss1A-3* double mutant line. At 2 wk after sowing on GM plates, it was already apparent that the double mutant had a very low germination rate. Although, in the
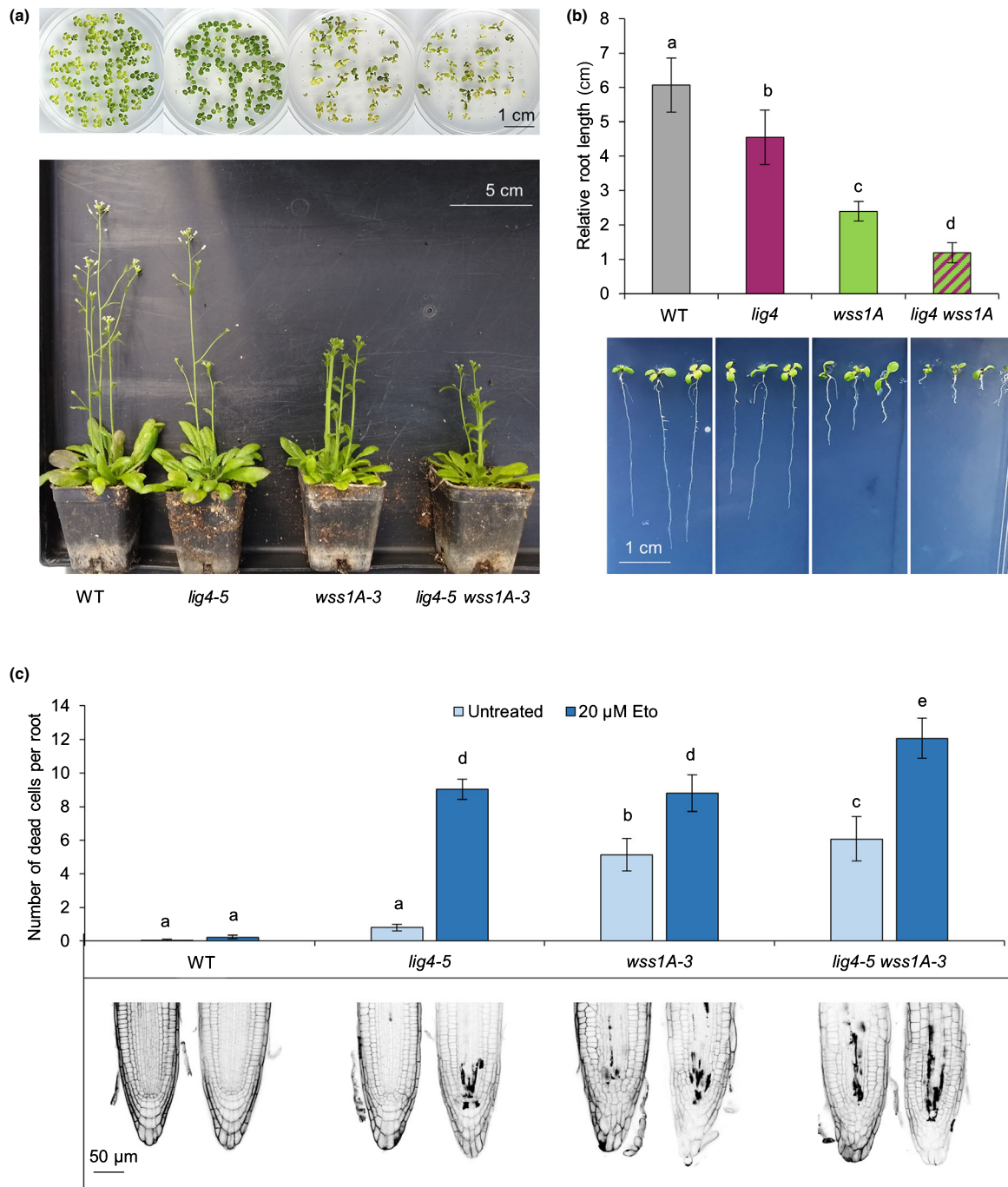
Fig. 3 Epistasis analysis of the *Arabidopsis thaliana lig4 wss1A* double mutant in growth, root length and Etoposide (Eto) sensitivity. (a) The *lig4-5 wss1A-3* double mutant displayed the same growth phenotype as the *wss1A-3* single mutant after 2 and 4 wk of cultivation. (b) Relative root length of 9-d-old seedlings (*n* = 3, *n* = 10). The *lig4-5 wss1A-3* double mutant exhibited significantly shorter roots than both single mutant lines and the WT. Statistical differences were calculated using a two-tailed *t*-test with unequal variances. (c) Number of dead cells per root of 5-d-old seedlings stained with propidium iodide (PI), uninduced and after treatment with 20 μM Eto (*n* = 3, *n* = 10). Both the untreated and treated roots of a genotype were compared to determine the Eto sensitivity, and the different genotypes, according to their treatment, were compared among each other. In the untreated condition, the *lig4-5 wss1A-3* double mutant displayed the same number of dead cells per root as the *wss1A-3* single mutant. However, after treatment with Eto, the double mutant showed a synergistic effect with a significantly enhanced number of dead cells per root compared with both single mutant lines. Statistical differences were calculated using a two-way ANOVA with Tukey's *post hoc* test. Error bars represent the standard deviation between the mean values of three biological replicates. Statistical differences were calculated using a two-tailed *t*-test with unequal variances and are presented as *a ≠ b* when *P* < 0.05. *n*, number of biological repeats; *N*, samples per biological repeat.

wss1A-3 mutant, still *c.* 60% of the seeds germinated, the double mutant line showed a germination rate of *c.* 9% (Fig. 4a). The germinated seedlings were planted and further cultivated. After *c.* 5 wk of cultivation in the glasshouse, the plants were characterized with regard to their growth phenotype. The *wss1A-3 teb-5* mutant showed a striking phenotype as it was significantly reduced in size compared with both single mutant lines. To analyze this even further, we performed a root length assay with the double mutant, in comparison to the single mutant lines and the WT (Fig. 4b). The *teb-5 wss1A-3* line, with a relative root length of *c.* 12% of that of the WT roots, showed statistically significantly shorter roots than the already short roots of the *teb-5* and the *wss1A-3* single mutant lines. These strong developmental defects are an indication that the double mutant has severe problems with cell division and replication, suggesting that both AtPOLQ and WSS1A are essential for maintaining genome integrity and that they work in parallel pathways that can partly complement each other. Unfortunately, as a result of the strong morphological defects of the *teb-5 wss1A-3* double mutant line, we were not able to challenge it with the topoisomerase inhibitor Eto.

Loss of *WSS1A* and *PolQ* leads to massive chromosome fragmentation

As the *teb-5 wss1A-3* double mutant line displayed more severe morphological defects than the *lig4-5 wss1A-3* line, we aimed to investigate this further on the cytological level by counting chromosomal aberrations occurring in somatic anaphases (Fig. 5). Surprisingly, the *teb-5* and the *lig4-5* single mutants showed a comparable number of defects to the WT but a lower number than the *wss1A-3* mutant. Anaphase defects in the *lig4-5 wss1A-3* double mutant were, if at all, only mildly increased in comparison to the *wss1A-3* single mutant. However, more unrepaired DSB were detected in the double mutant. By contrast, the *teb-5 wss1A-3* double mutant displayed a drastically elevated number of anaphase defects in comparison to all other mutant lines. Out of all counted anaphases in *teb-5 wss1A-3*, *c.* 15% showed chromosomal aberrations. Similar to the *lig4-5 wss1A-3* double mutant line, the proportion of chromosomal fragmentations, in particular, was strongly increased. Thus, our analysis clearly shows that in the absence of WSS1A, unrepaired DSBs arise – a
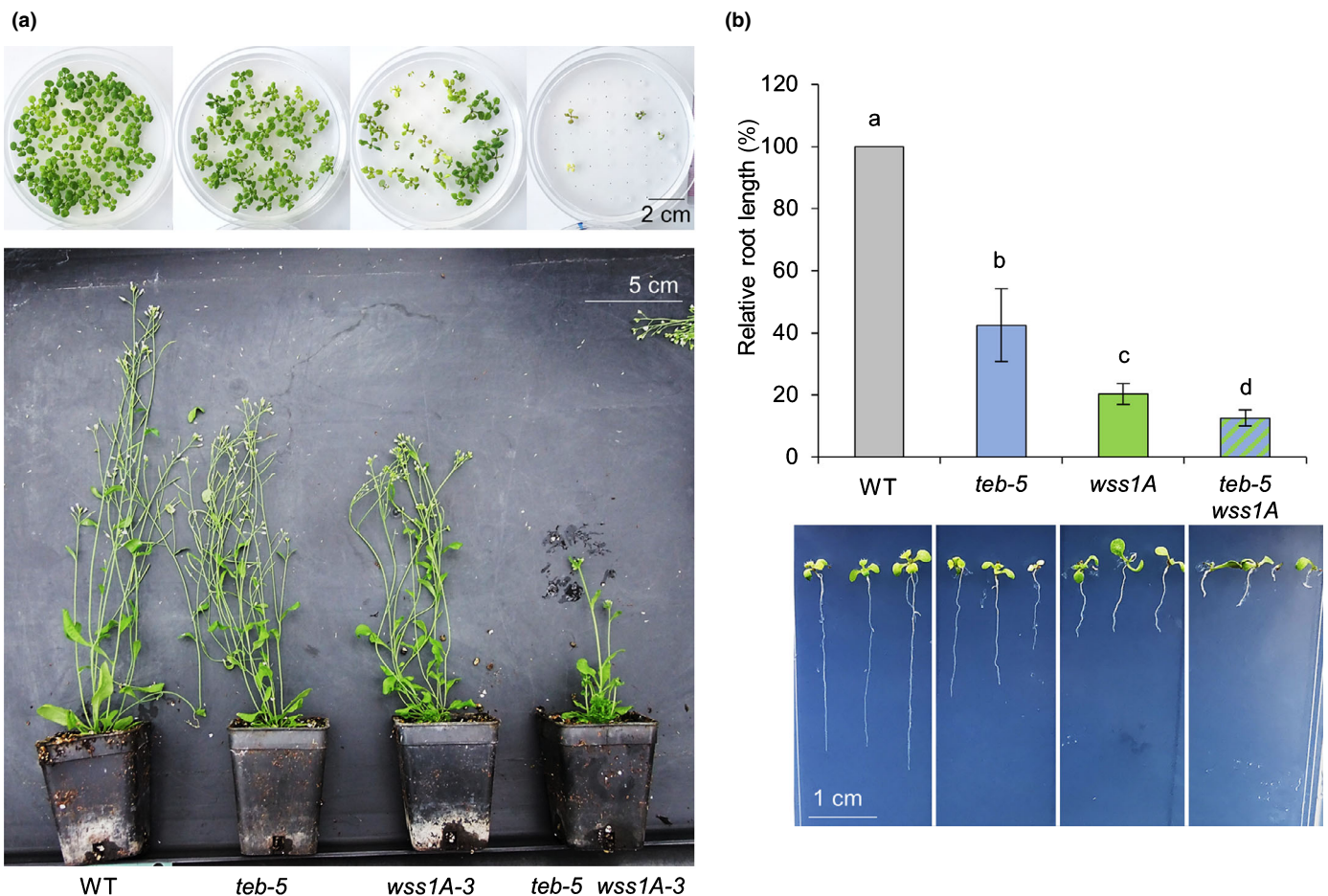

Fig. 4 Epistasis analysis of *Arabidopsis thaliana teb wss1A* double mutants. (a) Growth phenotypes of the different mutant lines in comparison to the wild-type after 2 and 5 wk of cultivation. The *teb-5 wss1A-3* exhibits severe developmental defects, with a strongly reduced germinate rate and growth. (b) Relative root length of 9-d-old seedlings (*n* = 3, *n* = 10). The *teb-5 wss1A-3* double mutant line displayed significantly shorter roots than both single mutant lines. Error bars represent the standard deviation between the mean values of three biological replicates. Statistical differences were calculated using a two-tailed *t*-test with unequal variances and are presented as *a* ≠ *b* when *P* < 0.05. *n*, number of biological repeats; *N*, samples per biological repeat.
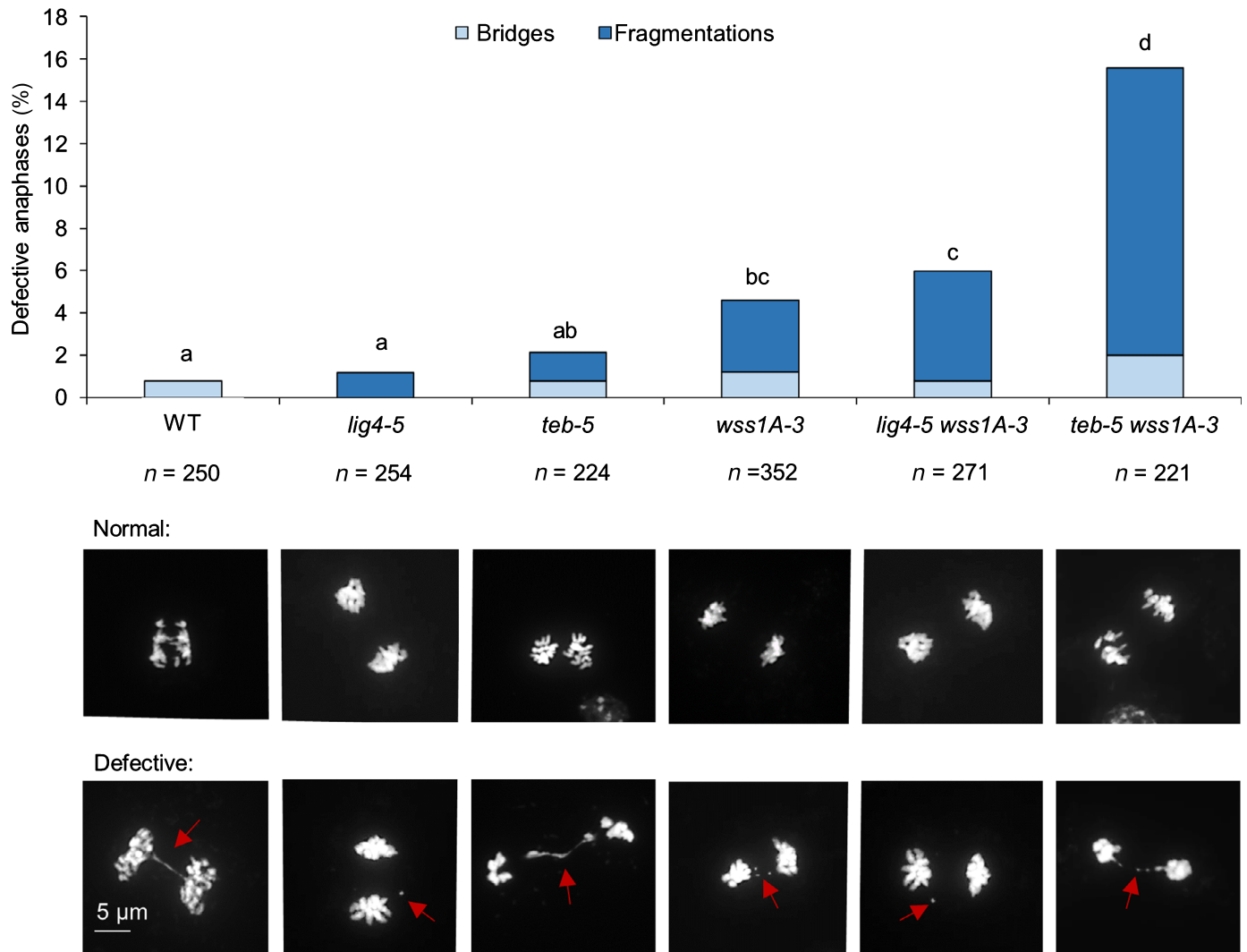
Fig. 5 Analysis of somatic anaphases of *Arabidopsis thaliana wss1A* and nonhomologous end joining (NHEJ) mutants. Percentage of defective anaphases in different mutant lines in comparison to the wild-type (WT). Chromatin spreads were stained with 4′,6-diamidino-2-phenylindole (DAPI) and visualized with epifluorescence microscopy. Defects (red arrows) were subdivided into anaphase bridges and chromosomal fragmentations. The *wss1A-3* single mutant showed significantly more defective anaphases compared with the WT and the *lig4-5* and *teb-5* single mutant lines. The *lig4-5 wss1A-3* double mutant showed the same number of defective anaphases as the *wss1A-3* single mutant, but a shift in the distribution of defects was observed as the *wss1A-3* mutant showed twice the amount of anaphase bridges compared with the *lig4-5 wss1A-3* double mutant. The *teb-5 wss1A-3* double mutant displayed significantly more defective anaphases than all other mutant lines. However, the distribution of defects was comparable to the *lig4-5 wss1A-3* double mutant line. Statistical differences were calculated using a two-tailed Fisher's exact test and are presented as $a \neq b$ when $P < 0.05$.

phenomenon that is further aggravated if cNHEJ or, in particular, aNHEJ pathways are not available for DSB repair. Thus, WSS1A is either directly involved in DSB repair in a pathway independent of cNHEJ and aNHEJ or suppresses the formation of persistent DSBs.

WSS1A is not required for the repair of CRISPR/Cas-induced DSB

In order to test whether WSS1A plays a direct role in DSB repair, we induced DSB in both WT plants and *wss1A* mutants, using the CRISPR/Cas9 systems from *Streptococcus pyogenes* (SpCas9) and *Staphylococcus aureus* (SaCas9) (Fauser *et al.*, 2014; Steinert *et al.*, 2015). Three targets were chosen for both nucleases. One is

located in a heterochromatic region (*TRANS*, At2G05640) while the other two are located in genes: *ADH1* (At1G77120) and *TT4* (At5G13930). Using deep sequencing, we analyzed and compared the quantity as well as the quality of DSB repair events in mutant and WT plants. The relative amount of reads with mutations was used to estimate the repair efficiency, as unrepaired DSBs cannot be amplified. Therefore, deficiencies in DSB repair would result in a relative increase of WT sequences. Two loci targeted with *Sa*Cas9, *ADH1* and *TRANS* showed a slight increase in the number of reads with mutations in the *wss1A* mutant of 1.1- and 1.2-fold, respectively (Table 1). Furthermore, we could observe an increased frequency of modified reads at two of the loci targeted with SpCas9 in the *wss1A* mutant plants compared with the WT control. While this increase is relatively weak

Table 1 Frequency of modified reads in *Arabidopsis thaliana* wild-type (WT) and mutant plants.

Cas-enzyme	Target	WT (total reads)	wss1A-3 (total reads)	Ratio
SaCas9	*ADH1*	52.91% (75 520)	59.81% (66 183)	1.1**
	TT4	87.92% (62 440)	88.88% (55 444)	1.0**
	TRANS	66.40% (79 029)	82.00% (91 526)	1.2**
SpCas9	*ADH1*	52.72% (61 402)	49.62% (48 889)	0.9**
	TT4	41.65% (45 670)	46.95% (30 816)	1.1**
	TRANS	50.69% (91 736)	69.94% (87 629)	1.4**

Next-generation sequence analysis was performed in WT and *wss1A-3* plants after Cas9-mediated cleavage of indicated target sequences. Depicted is the percentage of reads harboring mutations and the ratio of mutated reads in *wss1A-3* to WT plants. Statistical differences were calculated using χ^2 test (**, $P \le 0.001$).

at the *TT4* target (1.1-fold), it is slightly more pronounced at the *TRANS* target, showing a 1.4-fold increase.

Thus, WSS1A is not required for the repair of DSB generated by Cas9. By contrast, its absence might in some cases even slightly enhance repair efficiencies. As such an effect could also influence the product classes of the repair events, we performed a detailed analysis of the repair patterns. We compared the size and the relative frequencies of insertions and deletions as well as the relative amount of DSB repaired by using microhomologies in mutant and WT plants for both nucleases. However, despite the observed differences in mutagenesis frequency, no divergence between WT and mutant plants could be detected concerning distribution of deletions and insertions at any locus (Figs 6a; S3). Regarding the frequency of microhomology-mediated DSB repair, only a slight change could be observed in half of the samples in comparison to the WT control (Fig. 6b). Moreover, as one target showed a decrease while two showed an increase in microhomology use, no correlation with the mutant background was apparent. Furthermore, the largest observed difference in *wss1A*-mutants amounts to a reduction of only $1/13^{th}$ compared with the observed microhomology-mediated DSB repair frequency in WT plants. Taken together, no indication for a change in the use of the two NHEJ pathways in the mutant was found, as the operation of aNHEJ is correlated with an increased use of microhomologies and occurrence of larger deletions than cNHEJ. Thus, WSS1A is not required for general DSB repair in *A. thaliana*, nor is it influencing the repair outcome.

Discussion

Although most DNA repair pathways have been well characterized for decades, the relevance of DPC repair has only been discovered in recent years (Stingele *et al.*, 2014, 2017). Central to DPC repair in yeast is the DNA-dependent metalloprotease Wss1. Recently, we characterized the plant homolog WSS1A and were able to demonstrate that it plays essential roles in the repair of enzymatic and nonenzymatic DPCs (Enderle *et al.*, 2019a; Hacker *et al.*, 2021). Here, we further defined the role of WSS1A in preserving genome stability in Arabidopsis.

Loss of WSS1A results in genome instability

In our previous work, we showed that the loss of WSS1A is associated with growth defects and sensitivity against DNA-damaging agents, indicating that a lack of DPC repair results in genome instability. To further characterize how the knockout affects the nuclear genome, we analyzed somatic anaphases, as this allows for the detection of instabilities on the chromosome level. These analyses revealed that plants deficient in WSS1A indeed have an increased number of defective anaphases. In principle, two kinds of aberrations can be detected with such an assay: anaphase bridges and fragmented chromosomes. We were able to show that the increase of aberrations in the mutant is solely a result of fragmented chromosomes. This is a strong indication either that there is a defect in DSB repair itself or that the absence of WSS1A results in the occurrence of more DSBs or unrepairable DSBs. In somatic cells, DSBs arise mainly during replication which, if unrepaired, also result in proliferation defects. A sensitive maker for replication-associated genome instability is the amount of 45S rDNA repeats. rDNA gene clusters are among the most unstable regions of the genome (Kobayashi, 2008). In yeast, rDNA stability and copy number have previously been shown to be affected by replication stress (Salim *et al.*, 2017). In Arabidopsis, loss of important replicative DNA repair factors, such as RTEL1, RMI2 or FANCJB, results in a reduction of 45S rDNA repeats (Röhrig *et al.*, 2016; Dorn *et al.*, 2019). Replication of 45S rDNA repeats is more error-prone and time-consuming than replication of other parts of the genome as a result of the formation of secondary structures, such as G4s. As long as protein synthesis is assured, a reduction of rDNA copy numbers thus helps cells to counterbalance DNA replication defects. Interestingly, it has been shown that the majority of 45S rDNA repeats can be deleted without phenotypic consequences in Arabidopsis by using CRISPR/Cas9 (Lopez *et al.*, 2021). Our analysis revealed that the *wss1A* mutant indeed harbors a massively reduced amount of 45S rDNA repeats in comparison to the WT. This is a clear indication of a replicative DNA repair defect resulting from WSS1A loss.

WSS1A is required for replicative DNA repair

The RTR complex is an important caretaker of genome stability during replication. In Arabidopsis, the complex consist of the helicase RECQ4A, the topoisomerase TOP3α and the structural proteins RMI1 and RMI2 (Hartung *et al.*, 2007, 2008; Knoll *et al.*, 2014; Röhrig *et al.*, 2016). RECQ4A has been shown to be particularly important for somatic DNA repair, in part through its ability to regress replication forks (Schröpfer *et al.*, 2014b). Here, we could show that double mutants of *WSS1A* with all members of the RTR complex are embryolethal, indicating that the protease plays an important role in replicative DNA repair, thereby compensating defects in factors of the RTR complex. Interestingly, severe growth defects can also occur in Arabidopsis when mutants of the RTR complex are combined with a knockout of the endonuclease MUS81:
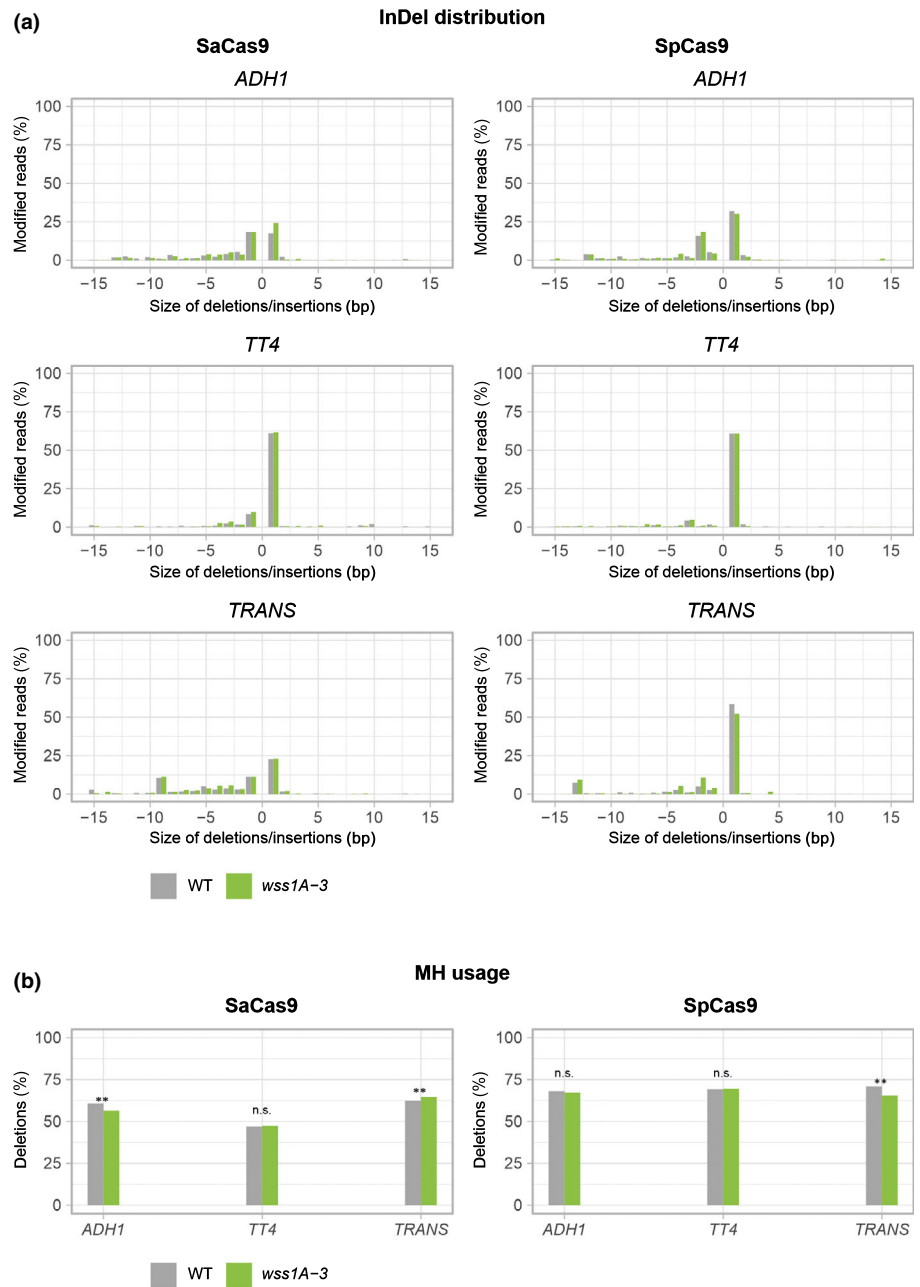
Fig. 6 Analysis of repair pattern of induced double-strand break (DSB). (a) Percentage of modified next-generation sequencing (NGS) reads showing insertions and deletions ranging from −15 to +15 bp at three different targets for SpCas9 and SaCas9 in *Arabidopsis thaliana* wild-type (WT) and *wss1A-3* mutants. (b) Frequency of deletion containing reads that show a repair pattern resulting from microhomology (MH)-mediated DSB repair. Statistical differences were calculated using χ^2 test (ns, $P > 0.01$; **, $P \leq 0.001$).

double mutants of *mus81 recq4A* germinated but were subsequently not viable, whereas *mus81 top3α* mutants were embryo-lethal (Hartung *et al.*, 2006; Dorn *et al.*, 2018). Thus, the replicative DNA repair functions of the RTR complex can be partially taken over by the endonuclease activity of MUS81 (Hartung *et al.*, 2007; Geuting *et al.*, 2009; Mannuss *et al.*, 2010; Dorn *et al.*, 2018). However, we assume that the protease and nuclease do not work in the same pathway to process aberrant replication intermediates, as our previous *in planta* analysis indicated that MUS81 is also able to process DPCs, but mostly in a parallel pathway to WSS1A (Enderle *et al.*, 2019a). Concerning the relationship of WSS1A and the components of the RTR complex, it was demonstrated in yeast and in worms that

double mutants deficient of the respective homologs Wss1/ DVC1 for WSS1A and Sgs1/HIM6 for RECQ4A exhibited synthetic lethality or reduced viability (Mullen *et al.*, 2011; Stingele *et al.*, 2016). For WSS1A and RTR homologs, essential functions in maintaining replication fork stability were demonstrated in yeast and mammals. ScWss1 is able to degrade histones, which assemble at long single-stranded DNA straps of stalled replication forks, and thus the replication fork can be restored (Maddi *et al.*, 2020). In humans, both RMI1 and the RECQ4A homolog BLM have been shown to interact with longer single-stranded DNA stretches coated by RPA. This promotes replication fork restart, possibly by resolving secondary structures of DNA that cause stalling (Shorrocks *et al.*, 2021).
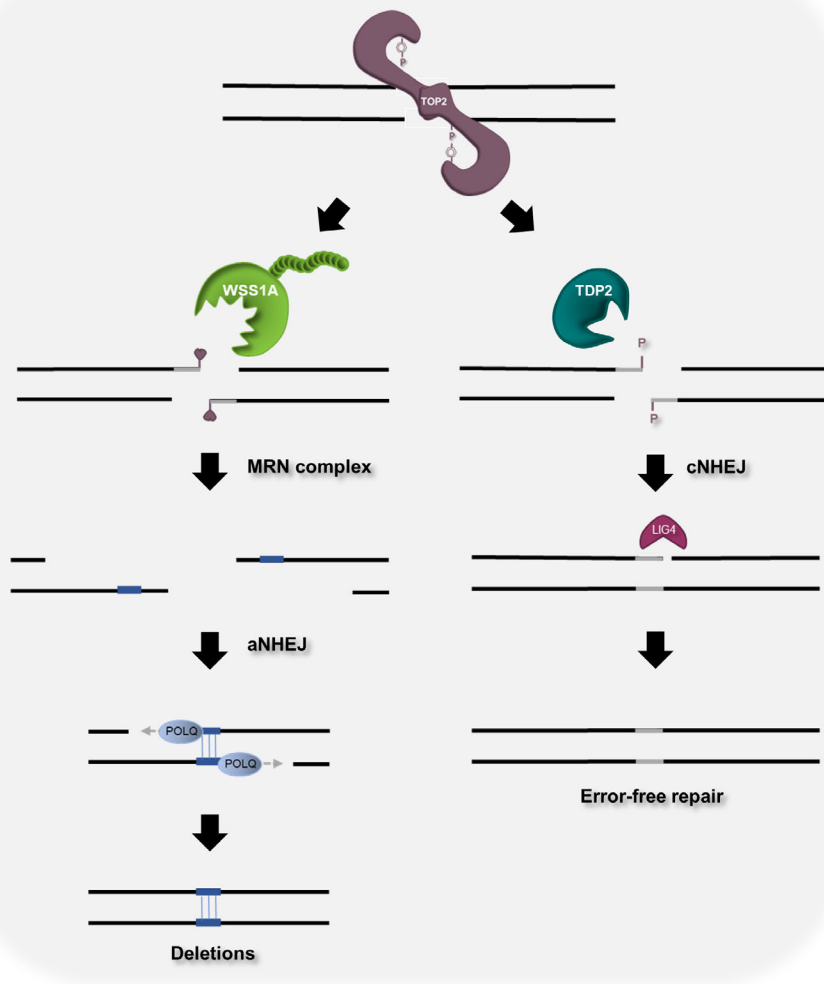
Fig. 7 WSS1A polishes DNA ends for subsequent double-strand break (DSB) repair. Topoisomerase 2 cleavage complexes (TOP2cc) can be repaired by two distinct mechanisms in plants. WSS1A can possibly degrade the protein part, thereby leaving only a small peptide remnant which, subsequently, has to be removed by the MRN complex. This results in a double-strand break (DSB) with longer 3′ overhangs that can only be repaired by the error-prone alternative nonhomologous end-joining (aNHEJ) pathway. WSS1A-mediated TOP2cc repair is therefore likely to involve the formation of deletions. However, TDP2, which is working in parallel to WSS1A, can hydrolyze the crosslink bond between TOP2 and the DNA, thereby generating a clean DSB. The DSB can be repaired by classical NHEJ (cNHEJ). As the DSB harbours 4 bp overhangs and 5′ phosphate residues, TOP2cc repair by TDP2 and subsequent cNHEJ is expected to be error-free.

WSS1A is not involved in DSB repair

The fact that the *wss1A* mutant displayed an elevated number of unrepaired chromosomal fragmentations indicated that WSS1A may also be required for DSB repair. DSB are primarily repaired by NHEJ mechanisms in plants (Puchta, 2005). Therefore, we were interested to investigate how the simultaneous loss of WSS1A and either the cNHEJ factor LIG4 or the aNHEJ factor POLQ would affect cell proliferation and DSB repair. The *lig4 wss1A* double mutant line exhibited a growth phenotype which was comparable to the *wss1A* single mutant and displayed only slightly more chromosome fragmentation than the *wss1A* mutant. However, the double mutant showed significantly shorter roots than the *wss1A* single mutant, indicating that LIG4 and WSS1A might partly compensate for each other in cell proliferation.

In contrast to the *lig4 wss1A* mutant, the *teb wss1A* double mutant displayed much more severe developmental defects, such as dwarfism and a strongly reduced root length. One reason for these defects might be the accumulation of chromosomal fragmentation in the cells of the double mutant. Indeed, the number of defective somatic anaphases was almost tripled in

comparison to the *wss1A* mutant (Fig. 5). These results indicated that WSS1A may indeed function in a DSB repair pathway parallel to POLQ. Alternatively, it might suppress persistent DSB formation.

To directly test whether WSS1A plays a role in DSB repair, we induced site-specific DSBs in the mutant as well as in WT plants using the CRISPR/Cas system. To avoid enzyme- or locus-specific effects, we induced breaks at three different loci located in eu- and heterochromatic regions with two different nucleases, *Sp*Cas9 and *Sa*Cas9. DSB repair was analyzed by deep sequencing using the number of mutated reads as mean for DSB repair efficiency and changes in repair patterns (size and position of insertions and deletions) as mean for determining the pathway choice. However, our analysis revealed no repair deficiency in *wss1A* mutant plants. Also, no changes in pathway choice were detectable for any locus. Interestingly, a slight increase in overall mutation frequency could be observed for more than half of the targets. A possible explanation for these results could be that WSS1A is able to degrade Cas9 under certain circumstances, as especially SpCas9 remains at the break site for a long time after cutting (Yourik *et al.*, 2019). Thus, in *wss1A* mutant plants, the
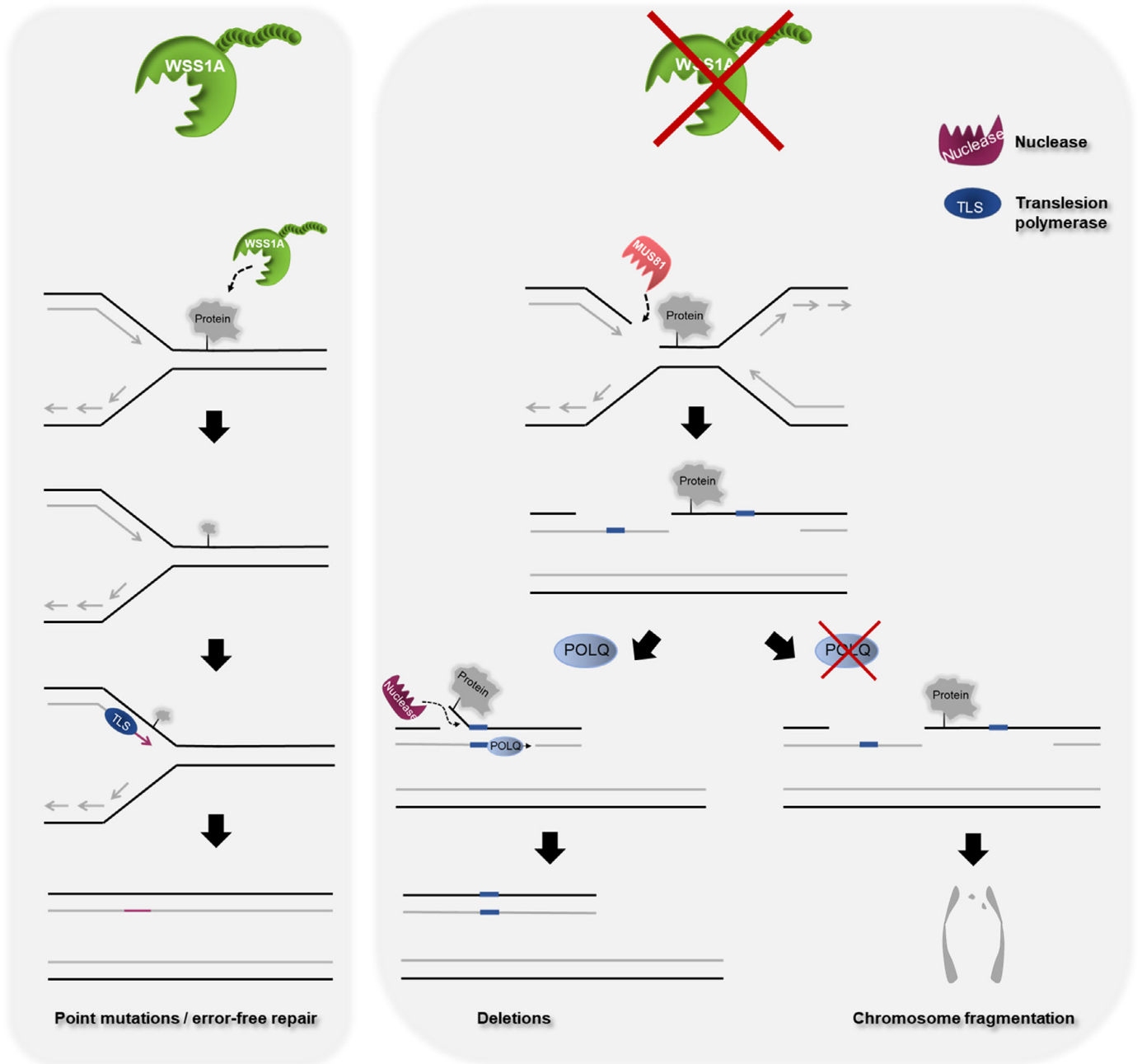
Fig. 8 WSS1A suppresses double-strand break (DSB) formation during replication. WSS1A can degrade proteinaceous obstacles at stalled replication forks, thereby leaving only a small peptide remnant that is subsequently bypassed by translesion polymerases. Incorrect insertion of bases by translesion synthesis might lead to either point mutations or error-free repair. If WSS1A is absent, stalled replication forks are mainly processed by MUS81 which generates an increased amount of one-sided DSBs. One-sided DSBs become two-sided by the arrival of the converging replication fork. Owing to the enhanced activity of the MRN complex in the S phase, the 5′ ends of the DSBs are resected, exposing microhomologies in the 3′ overhangs. These can subsequently anneal to each other. The heterologous 3′ flaps are removed by nucleases and POLQ promotes fill-in synthesis. This process is associated with the formation of deletions. However, if POLQ is absent as well, replication-associated DSBs are not repaired in time before the cell enters mitosis, leading to chromosome fragmentation during mitosis.

half-life of Cas9 might be slightly increased, leading to a prolonged period of time for potential DSB induction. However, even in this case, the analysis of the resulting repair patterns in *wss1A* mutants compared with WT plants revealed no significant changes, either in the distribution of deleted bases or in the size of the resulting indels. This suggests that in the *wss1A* mutant, both cNHEJ and aNHEJ are involved in DSB repair in the same

way as in the WT. Thus, WSS1A is neither involved in DSB repair itself nor is it influencing its outcome.

WSS1A suppresses formation of persisting DSB

These results indicate that although the amount of chromosomal fragmentation is elevated in the *wss1A* mutant, this is not a result

of a defect in DSB repair. In principle, there are two ways in which WSS1A could prevent the occurrence of unrepaired DSBs: either by suppressing DSB formation or by polishing DSB ends that would otherwise be unrepairable and would persist. We believe that WSS1A contributes in both ways to preserve genome stability.

Just recently, we were able to demonstrate that WSS1A does indeed have an important function in polishing unrepaired DSB ends so that they can be processed by the NHEJ machinery in the long run. TOP2cc are enzymatic DPCs formed upon an abortive reaction of TOP2, in which the catalytic reaction intermediate of TOP2 is trapped next to a DSB (Wang, 1996). We could show that TOP2cc can be repaired by two distinct mechanisms in plants (Hacker et al., 2021). One mechanism is based on the hydrolysis of the crosslink bond by the tyrosyl-DNA-phosphodiesterase 2 (TDP2) with subsequent DSB repair by error-free cNHEJ. We speculated that the other pathway involves proteolytic degradation of TOP2 by WSS1A. The remaining peptide remnants after WSS1A-mediated proteolysis most probably have to be removed by the MRN complex before the DSB can be re-ligated. As we were now able to show that the *wss1A lig4* double mutant was more sensitive against Eto than both single mutants, this indicates that both factors work in parallel pathways in TOP2cc repair (Fig. 3c). Thus, after WSS1A-mediated proteolysis of TOP2, these DSBs are most likely mainly repaired by aNHEJ (Fig. 7).

As this pathway is supposed to be error-prone, we can only speculate that in the G1 and G2 phases, TOP2cc are preferentially repaired by TDP2 and subsequent error-free cNHEJ, whereas WSS1A might be more important during replication. However, if both pathways are unavailable, TOP2cc might not be repaired in time before entering cell division, thus resulting in chromosomal alterations and fragmentation.

On the other side, the strong genetic interaction of *WSS1A* with factors of the RTR complex is an indication that WSS1A can protect stalled replication forks and helps them to restart. In addition, it might also be involved in the removal of complex replication-blocking lesions. By contrast, if stalled replication forks are processed by endonucleases, complex DSBs might arise, which are unsuitable for cNHEJ and are thus most commonly repaired by aNHEJ (Wang et al., 2019; Nisa et al., 2021). In the absence of WSS1A, the number of these DSBs could increase greatly, overstraining the capacity of the NHEJ pathways to repair all breaks in time before the cell enters mitosis (Fig. 8).

This would explain the massive increase of unrepaired DSBs in the corresponding *teb wss1A* double mutant. Thus, in WT plants, WSS1A is able to suppress aberrant DSB formation by directly removing the replication-stalling obstacle or by protecting the stalled replication forks (Stingele et al., 2014; Enderle et al., 2019a; Maddi et al., 2020). We assume that the DSB-preventing function during replication is a conserved feature of WSS1A homologs in general. Indeed, for SPRTN, the functional Wss1 homolog in humans, a central role in ensuring the progression of replications forks was shown and, in its absence, S-phase-specific DSBs arise after DPC induction (Vaz et al., 2016). In yeast cells, loss of Wss1 results in accumulation of gross chromosomal

rearrangements that were postulated to arise from the repair of replication-associated, aberrant single-ended DSBs (Stingele et al., 2014).

In summary, our results demonstrate that WSS1A plays an absolutely crucial role in maintaining genome integrity in plants, especially during replication, by preventing the occurrence of persistent DSB.

Author contributions

JE, AD and HP designed the research. LH, NC, LF and JE performed the research. LH, NC, LF, AD and HP carried out the data analysis. LH, NC, LF, AD and HP wrote the manuscript.

ORCID

Niklas Capdeville https://orcid.org/0000-0001-6512-0466
Annika Dorn https://orcid.org/0000-0002-0749-8425
Janina Enderle-Kukla https://orcid.org/0000-0002-7016-0064
Leonie Hacker https://orcid.org/0000-0002-6912-0022
Holger Puchta https://orcid.org/0000-0003-1073-8546

Data availability

The data that support the findings of this study are available from the corresponding author upon reasonable request. Next-generation sequencing data that support the finding of this study have been deposited in SRA (accession no. PRJNA777556).

References

Arana ME, Seki M, Wood RD, Rogozin IB, Kunkel TA. 2008. Low-fidelity DNA synthesis by human DNA polymerase theta. *Nucleic Acids Research* **36**: 3847–3856.

Chan SH, Yu AM, McVey M. 2010. Dual roles for DNA polymerase theta in alternative end-joining repair of double-strand breaks in Drosophila. *PLoS Genetics* **6**: e1001005.

Chang HHY, Pannunzio NR, Adachi N, Lieber MR. 2017. Non-homologous DNA end joining and alternative pathways to double-strand break repair. *Nature Reviews. Molecular Cell Biology* **18**: 495–506.

Clement K, Rees H, Canver MC, Gehrke JM, Farouni R, Hsu JY, Cole MA, Liu DR, Joung JK, Bauer DE et al. 2019. CRISPResso2 provides accurate and rapid genome editing sequence analysis. *Nature Biotechnology* **37**: 224–226.

Clough SJ, Bent AF. 1998. Floral dip: a simplified method for Agrobacterium-mediated transformation of *Arabidopsis thaliana*. *The Plant Journal* **16**: 735–743.

Dorn A, Feller L, Castri D, Röhrig S, Enderle J, Herrmann NJ, Block-Schmidt A, Trapp O, Köhler L, Puchta H. 2019. An Arabidopsis FANCJ helicase homologue is required for DNA crosslink repair and rDNA repeat stability. *PLoS Genetics* **15**: e1008174.

Dorn A, Röhrig S, Papp K, Schröpfer S, Hartung F, Knoll A, Puchta H. 2018. The topoisomerase 3α zinc-finger domain T1 of *Arabidopsis thaliana* is required for targeting the enzyme activity to Holliday junction-like DNA repair intermediates. *PLoS Genetics* 14: e1007674.

Enderle J, Dorn A, Beying N, Trapp O, Puchta H. 2019a. The protease WSS1A, the endonuclease MUS81, and the phosphodiesterase TDP1 are involved in independent pathways of DNA-protein crosslink repair in plants. *Plant Cell* 31: 775–790.

Enderle J, Dorn A, Puchta H. 2019b. DNA- and DNA-protein-crosslink repair in plants. *International Journal of Molecular Sciences* 20: 4304.

Fauser F, Schiml S, Puchta H. 2014. Both CRISPR/Cas-based nucleases and nickases can be used efficiently for genome engineering in *Arabidopsis thaliana*. *The Plant Journal* 79: 348–359.

Fulton TM, Chunwongse J, Tanksley SD. 1995. Microprep protocol for extraction of DNA from tomato and other herbaceous plants. *Plant Molecular Biology Reporter* 13: 207–209.

Geuting V, Kobbe D, Hartung F, Dürr J, Focke M, Puchta H. 2009. Two distinct MUS81-EME1 complexes from Arabidopsis process Holliday junctions. *Plant Physiology* 150: 1062–1071.

Hacker L, Dorn A, Enderle J, Puchta H. 2021. The repair of topoisomerase 2 cleavage complexes in Arabidopsis. *The Plant Cell*: koab228.

Hacker L, Dorn A, Puchta H. 2020. Repair of DNA-protein crosslinks in plants. *DNA Repair* 87. doi: 10.1016/j.dnarep.2020.102787.

Hartung F, Suer S, Bergmann T, Puchta H. 2006. The role of AtMUS81 in DNA repair and its genetic interaction with the helicase AtRecQ4A. *Nucleic Acids Research* 34: 4438–4448.

Hartung F, Suer S, Knoll A, Wurz-Wildersinn R, Puchta H. 2008. Topoisomerase 3alpha and RMI1 suppress somatic crossovers and are essential for resolution of meiotic recombination intermediates in *Arabidopsis thaliana*. *PLoS Genetics* 4: e1000285.

Hartung F, Suer S, Puchta H. 2007. Two closely related RecQ helicases have antagonistic roles in homologous recombination and DNA repair in *Arabidopsis thaliana*. *Proceedings of the National Academy of Sciences, USA* 104: 18836–18841.

Ide H, Shoulkamy MI, Nakano T, Miyamoto-Matsubara M, Salem AMH. 2011. Repair and biochemical effects of DNA-protein crosslinks. *Mutation Research* 711: 113–122.

Inagaki S, Suzuki T, Ohto M, Urawa H, Horiuchi T, Nakamura K, Morikami A. 2006. Arabidopsis TEBICHI, with helicase and DNA polymerase domains, is required for regulated cell division and differentiation in meristems. *Plant Cell* 18: 879–892.

Ira G, Pellicioli A, Balijja A, Wang X, Fiorani S, Carotenuto W, Liberi G, Bressan D, Wan L, Hollingsworth NM *et al.* 2004. DNA end resection, homologous recombination and DNA damage checkpoint activation require CDK1. *Nature* 431: 1011–1017.

Klemm T, Mannuß A, Kobbe D, Knoll A, Trapp O, Dorn A, Puchta H. 2017. The DNA translocase RAD5A acts independently of the other main DNA repair pathways, and requires both its ATPase and RING domain for activity in *Arabidopsis thaliana*. *The Plant Journal* 91: 725–740.

Knoll A, Puchta H. 2011. The role of DNA helicases and their interaction partners in genome stability and meiotic recombination in plants. *Journal of Experimental Botany* 62: 1565–1579.

Knoll A, Schröpfer S, Puchta H. 2014. The RTR complex as caretaker of genome stability and its unique meiotic function in plants. *Frontiers in Plant Science* 5:33.

Kobayashi T. 2008. A new role of the rDNA and nucleolus in the nucleus–rDNA instability maintains genome integrity. *BioEssays* 30: 267–272.

Liang L, Deng L, Nguyen SC, Zhao X, Maulion CD, Shao C, Tischfield JA. 2008. Human DNA ligases I and III, but not ligase IV, are required for microhomology-mediated end joining of DNA double-strand breaks. *Nucleic Acids Research* 36: 3297–3310.

Lobet G, Pagès L, Draye X. 2011. A novel image-analysis toolbox enabling quantitative analysis of root system architecture. *Plant Physiology* 157: 29–39.

Lopez FB, Fort A, Tadini L, Probst AV, McHale M, Friel J, Ryder P, Pontvianne FDR, Pesaresi P, Sulpice R *et al.* 2021. Gene dosage compensation of rRNA transcript levels in *Arabidopsis thaliana* lines with reduced ribosomal gene copy number. *Plant Cell* 33: 1135–1150.

Maddi K, Sam DK, Bonn F, Prgomet S, Tulowetzke E, Akutsu M, Lopez-Mosqueda J, Dikic I. 2020. Wss1 promotes replication stress tolerance by degrading histones. *Cell Reports* 30: 3117–3126.

Mannuss A, Dukowic-Schulze S, Suer S, Hartung F, Pacher M, Puchta H. 2010. RAD5A, RECQ4A, and MUS81 have specific functions in homologous recombination and define different pathways of DNA repair in *Arabidopsis thaliana*. *Plant Cell* 22: 3318–3330.

Mullen JR, Das M, Brill SJ. 2011. Genetic evidence that polysumoylation bypasses the need for a SUMO-targeted Ub ligase. *Genetics* 187: 73–87.

Nisa M, Bergis C, Pedroza-Garcia J-A, Drouin-Wahbi J, Mazubert C, Bergounioux C, Benhamed M, Raynaud C. 2021. The plant DNA polymerase theta is essential for the repair of replication-associated DNA damage. *The Plant Journal* 106: 1197–1207.

Nishizawa-Yokoi A, Saika H, Hara N, Lee L-Y, Toki S, Gelvin SB. 2021. Agrobacterium T-DNA integration in somatic cells does not require the activity of DNA polymerase θ. *New Phytologist* 229: 2859–2872.

Park J, Lim K, Kim J-S, Bae S. 2017. Cas-analyzer: an online tool for assessing genome editing results using NGS data. *Bioinformatics* 33: 286–288.

Plank JL, Wu J, Hsieh T-S. 2006. Topoisomerase IIIalpha and Bloom's helicase can resolve a mobile double Holliday junction substrate through convergent branch migration. *Proceedings of the National Academy of Sciences, USA* 103: 11118–11123.

Puchta H. 2005. The repair of double-strand breaks in plants: mechanisms and consequences for genome evolution. *Journal of Experimental Botany* 56: 1–14.

Raynard S, Bussen W, Sung P. 2006. A double Holliday junction dissolvasome comprising BLM, topoisomerase IIIalpha, and BLAP75. *Journal of Biological Chemistry* 281: 13861–13864.

Recker J, Knoll A, Puchta H. 2014. The *Arabidopsis thaliana* homolog of the helicase RTEL1 plays multiple roles in preserving genome stability. *Plant Cell* 26: 4889–4902.

Röhrig S, Schröpfer S, Knoll A, Puchta H. 2016. The RTR complex partner RMI2 and the DNA helicase RTEL1 are both independently involved in preserving the stability of 45S rDNA repeats in *Arabidopsis thaliana*. *PLoS Genetics* 12: e1006394.

Ross KJ, Fransz P, Jones GH. 1996. A light microscopic atlas of meiosis in *Arabidopsis thaliana*. *Chromosome Research* 4: 507–516.

Salim D, Bradford WD, Freeland A, Cady G, Wang J, Pruitt SC, Gerton JL. 2017. DNA replication stress restricts ribosomal DNA copy number. *PLoS Genetics* 13: e1007006.

Sargent RG, Brenneman MA, Wilson JH. 1997. Repair of site-specific double-strand breaks in a mammalian chromosome by homologous and illegitimate recombination. *Molecular and Cellular Biology* 17: 267–277.

Schmidt C, Pacher M, Puchta H. 2019. DNA break repair in plants and its application for genome engineering. *Methods in Molecular Biology* 1864: 237–266.

Schrempf A, Slyskova J, Loizou JI. 2021. Targeting the DNA repair enzyme polymerase θ in cancer therapy. *Trends in Cancer* 7: 98–111.

Schröpfer S, Knoll A, Trapp O, Puchta H. 2014a. DNA repair and recombination in plants. In: Howell SH, ed. *Molecular biology*. New York, NY, USA: Springer, 51–93.

Schröpfer S, Kobbe D, Hartung F, Knoll A, Puchta H. 2014b. Defining the roles of the N-terminal region and the helicase activity of RECQ4A in DNA repair and homologous recombination in Arabidopsis. *Nucleic Acids Research* 42: 1684–1697.

Seol J-H, Shim EY, Lee SE. 2018. Microhomology-mediated end joining: good, bad and ugly. *Mutation Research* 809: 81–87.

Shorrocks A-MK, Jones SE, Tsukada K, Morrow CA, Belblidia Z, Shen J, Vendrell I, Fischer R, Kessler BM, Blackford AN. 2021. The Bloom syndrome complex senses RPA-coated single-stranded DNA to restart stalled replication forks. *Nature Communications* 12: 585.

Steinert J, Schiml S, Fauser F, Puchta H. 2015. Highly efficient heritable plant genome engineering using Cas9 orthologues from *Streptococcus thermophilus* and *Staphylococcus aureus*. *The Plant Journal* 84: 1295–1305.

Stingele J, Bellelli R, Alte F, Hewitt G, Sarek G, Maslen S, Tsutakawa S, Borg A, Kjær S, Tainer J *et al.* 2016. Mechanism and regulation of DNA-protein crosslink repair by the DNA-dependent metalloprotease SPRTN. *Molecular Cell* 64: 688–703.

Stingele J, Bellelli R, Boulton SJ. 2017. Mechanisms of DNA-protein crosslink repair. *Nature Reviews. Molecular Cell Biology* 18: 563–573.

Stingele J, Schwarz MS, Bloemeke N, Wolf PG, Jentsch S. 2014. A DNA-dependent protease involved in DNA-protein crosslink repair. *Cell* 158: 327–338.

Szostak JW, Orr-Weaver TL, Rothstein RJ, Stahl FW. 1983. The double-strand-break repair model for recombination. *Cell* 33: 25–35.

van Kregten M, de Pater S, Romeijn R, van Schendel R, Hooykaas PJJ, Tijsterman M. 2016. T-DNA integration in plants results from polymerase-θ-mediated DNA repair. *Nature Plants* 2: 16164.

van Schendel R, van Heteren J, Welten R, Tijsterman M. 2016. Genomic scars generated by polymerase theta reveal the versatile mechanism of alternative end-joining. *PLoS Genetics* 12: e1006368.

Vaz B, Popovic M, Newman JA, Fielden J, Aitkenhead H, Halder S, Singh AN, Vendrell I, Fischer R, Torrecilla I *et al.* 2016. Metalloprotease SPRTN/DVC1 orchestrates replication-coupled DNA-protein crosslink repair. *Molecular Cell* 64: 704–719.

Wang JC. 1996. DNA topoisomerases. *Annual Review of Biochemistry* 65: 635–692.

Wang Z, Song Y, Li S, Kurian S, Xiang R, Chiba T, Wu X. 2019. DNA polymerase θ (POLQ) is important for repair of DNA double-strand breaks caused by fork collapse. *Journal of Biological Chemistry* 294: 3909–3919.

Waterworth WM, Masnavi G, Bhardwaj RM, Jiang Q, Bray CM, West CE. 2010. A plant DNA ligase is an important determinant of seed longevity. *The Plant Journal* 63: 848–860.

Wu L, Hickson ID. 2003. The Bloom's syndrome helicase suppresses crossing over during homologous recombination. *Nature* 426: 870–874.

Yourik P, Fuchs RT, Mabuchi M, Curcuru JL, Robb GB. 2019. Staphylococcus aureus Cas9 is a multiple-turnover enzyme. *RNA* 25: 35–44.

Zhao B, Rothenberg E, Ramsden DA, Lieber MR. 2020. The molecular basis and disease relevance of non-homologous DNA end joining. *Nature Reviews. Molecular Cell Biology* 21: 765–781.

Supporting Information

Additional Supporting Information may be found online in the Supporting Information section at the end of the article.

Fig. S1 Embryo lethality of *Arabidopsis thaliana rmi1 wss1A* double mutant lines.

Fig. S2 Defective embryo development in *Arabidopsis thaliana rmi1 wss1A* double mutant lines.

Fig. S3 Distribution of deleted bases.

Table S1 Sequences of the used oligonucleotides.

Table S2 Primer combinations for genotyping.

Table S3 Primer combinations used for qPCR analysis.

Table S4 Oligonucleotides used as spacers.

Table S5 Oligonucleotides for NGS amplicon generation.

Please note: Wiley Blackwell are not responsible for the content or functionality of any Supporting Information supplied by the authors. Any queries (other than missing material) should be directed to the *New Phytologist* Central Office.

About *New Phytologist*

- *New Phytologist* is an electronic (online-only) journal owned by the New Phytologist Foundation, a **not-for-profit organization** dedicated to the promotion of plant science, facilitating projects from symposia to free access for our Tansley reviews and Tansley insights.

- Regular papers, Letters, Viewpoints, Research reviews, Rapid reports and both Modelling/Theory and Methods papers are encouraged. We are committed to rapid processing, from online submission through to publication 'as ready' via *Early View* – our average time to decision is <26 days. There are **no page or colour charges** and a PDF version will be provided for each article.

- The journal is available online at Wiley Online Library. Visit **www.newphytologist.com** to search the articles and register for table of contents email alerts.

- If you have any questions, do get in touch with Central Office (np-centraloffice@lancaster.ac.uk) or, if it is more convenient, our USA Office (np-usaoffice@lancaster.ac.uk)

- For submission instructions, subscription and all the latest information visit **www.newphytologist.com**